American Mineralogist, Volume 91, pages 1831–1838, 2006

Does antigorite really contain 4- and 8-membered rings of tetrahedra?

István Dódony,[1,*] Mihály Pósfai,[2] and Peter R. Buseck[1]

[1]Departments of Geological Sciences and Chemistry/Biochemistry, Arizona State University, Tempe, Arizona 85287, U.S.A.
[2]Department of Earth and Environmental Sciences, Pannon University, Veszprém, POB 158, H-8200 Hungary

Abstract

Recent studies of the structure of antigorite by Capitani and Mellini (2004, 2005) and by us (Dódony et al. 2002; Dódony and Buseck 2004a) produced contradictory results. The main point of contention is whether 4- and 8-membered rings of tetrahedra occur at the positions where the tetrahedra in the tetrahedral sheets reverse their orientation. We analyzed electron diffraction patterns and transmission electron microscopy images in the paper of Capitani and Mellini (2005) and found no evidence for 4- and 8-membered rings of tetrahedra. On the contrary, we show that their TEM data confirm our antigorite model (Dódony et al. 2002) for the $m = 16$ structure. The significance of this debate goes beyond the subtleties of the structure of antigorite and highlights ambiguities in interpretation of HRTEM images as well as problems that can arise during image processing.

Keywords: Serpentine, antigorite, crystal structure, HRTEM, electron diffraction, image processing

Introduction

Several recent papers discuss the structure of antigorite (Dódony et al. 2002; Grobéty 2003; Capitani and Mellini 2004, 2005; Dódony and Buseck 2004a). An X-ray single-crystal structure refinement by Capitani and Mellini (2004) resulted in a structure model that is basically identical to that of Uehara and Shirozu (1985). The X-ray results were complemented by high-resolution transmission electron microscopy (HRTEM) images and selected-area electron diffraction (SAED) patterns in a subsequent paper (Capitani and Mellini 2005; hereafter referred to as CM). This TEM study prompted us to reexamine our previous results (Dódony et al. 2002) and to scrutinize the interpretations in CM.

The antigorite structure consists of alternating tetrahedral (**T**) silicate and octahedral (**O**) sheets of Mg coordinated to oxygen and hydroxyls. The major focus of the present paper lies in the positions where the polarities of the tetrahedra in the **T** sheets reverse. These structural reversals are important in antigorite, as well as in certain other modulated structures, because they provide insights into how crystals accommodate small dimensional differences caused by subtle changes in composition (Perbost et al. 2003). The heart of the controversy is whether, in addition to the 6-membered silicate rings typical of phyllosilicates, there are additional 4- and 8-membered silicate rings. The positions of these rings were called "8-reversals" for brevity by Capitani and Mellini (2004) and we adopt this terminology.

The positions of reversals are best visible in planes perpendicular to the crystallographic **a** axis, and these contain 4- and 8-membered silicate rings in most models, but only 6-membered rings in the models of Dódony et al. (2002)[1] (Fig. 1). The difference figures prominently in the model of CM. It would seem that resolution of this difference would be simple, but we shall show that it requires great care.

We think the conflicting results were caused by misinterpretations of TEM data and the results of image processing. Although we did not have a chance to measure the sample studied by CM, the good quality and high resolution of their figures (a preprint was kindly provided by M. Mellini) allowed us to perform calculations using their data[2]. The purposes of our paper are to present revised interpretations of their TEM results and processed images, to resolve the dispute over the structure of antigorite and, in the process, to provide a type study of the use of HRTEM images to test data from X-ray diffraction for certain complex structures.

Experimental vs. calculated SAED patterns

Comparison of calculated and experimental SAED patterns can confirm the validity of the structure models used for calculations. A good match of spacings and angles between experimental and calculated diffraction patterns is a necessary test of an accurate model. There are significant differences in measurements of CM and those made by us using their X-ray and TEM results. The value deduced from [–210] projections in Figures 15 and 16

* Permanent address: Department of Mineralogy, Eötvös L. University, Budapest, H-1117, Pázmány sétány 1C, Hungary. E-mail: dodony@t-online.hu

[1] Dódony et al. (2002) discussed several related models for the various antigorites having different modulation wavelengths and stackings. The models differ in numbers of polyhedral units, but the basic structural features are the same in all of them.

[2] We used the Cerius[2] 4.0 software (Molecular Simulation Institute, Inc.) for simulating HRTEM images and SAED patterns, and Digital Micrograph 2.5.7 (Meyer et al. 1996) for image filtering.

0003-004X/06/1112–1831$05.00/DOI: 10.2138/am.2006.1971

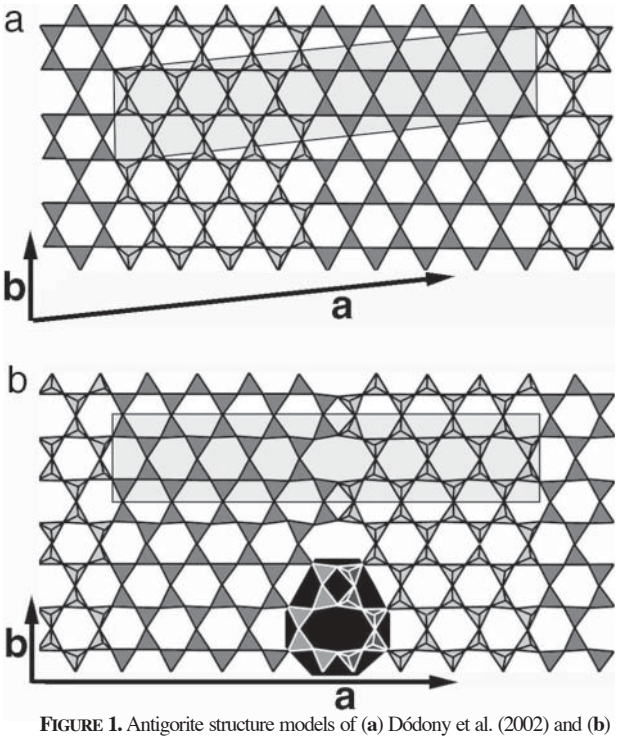

FIGURE 1. Antigorite structure models of (**a**) Dódony et al. (2002) and (**b**) Capitani and Mellini (2004) viewed down **c***. The two models differ mainly in the **T** sheets. The 4- and 8-membered silicate rings assumed by CM are present in **b** and highlighted in the black box, but they are missing in **a**. A unit cell is marked in both **a** and **b**.

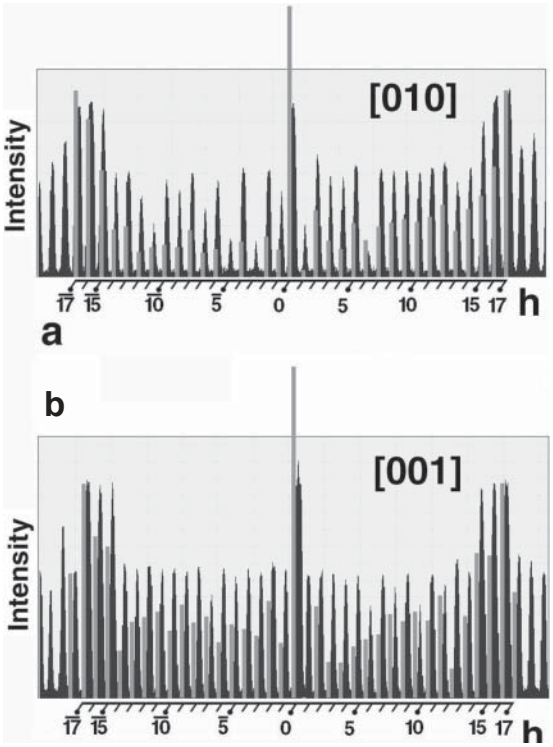

FIGURE 2. Comparison of *h*00 SAED intensities calculated by CM (black) and in this study (gray) using the structure model of Capitani and Mellini (2004) for (**a**) [010] and (**b**) [001] projections. Significant differences exist between corresponding intensity ratios.

of CM is 69°, instead of their published β-value of 91.3°. CM reported their sample as an $m = 17$ antigorite, but we find their images and SAED patterns correspond to an $m = 16$ antigorite. Significant variations exist for the unit-cell parameters and raise questions about the structure model.

Structural details within the unit cell are reflected by intensity distributions in diffraction patterns. Supercell reflections in Figures 2b and 3b of CM are intense, but they are weak in our calculations (Fig. 2). The many differences likely result from data processing by CM. We assume that CM chose an upper intensity limit, and that intensities above this limit were truncated to improve the visibility of weak reflections produced by the modulations. The remaining data were then presumably rescaled to the intensity range available for graphical representation. However, this procedure can lead to serious problems. When we followed this procedure using their data, we had to truncate their most intense reflections by two orders of magnitude to show the weakest reflections, and they then had misleadingly uniform intensities.

The intensities in calculated SAED patterns in CM are drastically truncated and are not compatible with experimental patterns. We believe that such truncated SAED patterns are misleading. We also found a poor match between data calculated based on the Capitani and Mellini (2004) antigorite model and

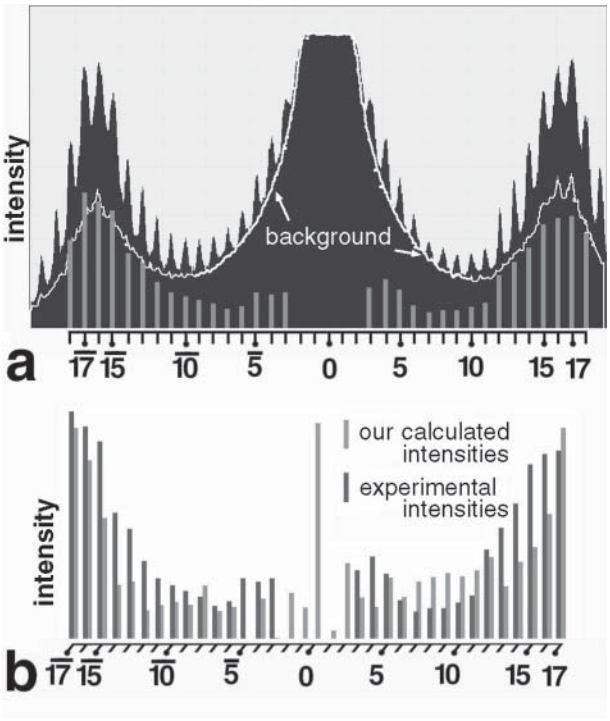

FIGURE 3. Intensity distributions measured along **a*** in Figure 2a of CM. (**a**) The profile defined by the black field indicates the experimental intensities of CM. The white curve is the background intensity. The difference, i.e., the background-subtracted signal, is given by the gray bars. (**b**) Comparison of the CM experimental data to our calculated intensities along **a***, normalized to each other using the $h = \pm 17$ reflections. Our calculations (for 200 kV and sample thickness of 100 Å) are based on structural data from Capitani and Mellini (2004).

their experimental SAED patterns (Fig. 3). The experimental and calculated $h00$ ($-17 > h > 17$) intensities show major differences, indicating that the experimental and model structures differ.

VISIBILITY OF STRUCTURAL DETAILS IN HRTEM IMAGES

[010] projections and site resolution

[010] HRTEM images show fundamental features of antigorite such as the **a**/**c** ratio, β, and the number of projected columns of cations in unit cells. Calculated images in Figure 4 of CM reveal a resolution of 2.5 Å that permits the discrimination of **T** and **O** positions. CM concluded that their [010] images, recorded under optimal experimental conditions and with limited beam damage, show good matches with simulated images. However, their processed experimental images contain artifacts that seriously limit and modify the structural information that can be extracted from them.

The Fourier transform (FT) of an image is a two-dimensional data set, every point of which is characterized by a complex number with amplitude and phase. The conventional representation of an FT shows its amplitude values, and in the FT of a raw image one can mask undesired details. Reconstruction of a raw image with selected components (comparable to reflections in a diffraction pattern) of its FT is called Fourier filtering and can be useful for enhancing periodic features in images.

Figure 5b of CM is reported as a Fourier-filtered image of Figure 5a of CM; however, the FT of their Figure 5b is not a subset of the FT of their Figure 5a. Our Figure 4 shows FTs of Figures 5a and 5b of CM and their amplitude profiles along $h00$, $h01$, and $h02$ lines. The brightness of the spots in Figure 4a and the corresponding spots in Figure 4b differ from each other and, moreover, there are additional spots in Figure 4b that are absent from the FT of the raw image. These differences were produced through image processing when CM produced their Figure 5b from their Figure 5a. Thus, Figure 5b of CM cannot be regarded as accurate. We find that the filtered HRTEM images in Figures 6 and 13 of CM also contain artifacts. Such filtered images are not suitable for structure analysis, despite the high quality of the original, raw images.

We measured structural data for the crystal in Figure 5a of CM (reproduced in our Fig. 5a). The image magnification was calibrated to the $d_{(001)}$ value. We performed repeated lattice refinements on the FT of their image using CRISP software for electron crystallography (Hovmöller 1992). Automatic peak finding and unit-cell refinement failed. After this trial, selected pairs of sharp, intense, non-collinear components were indexed and used for the calculation of starting unit-cell parameters. The results show a β value of 95.00° (±0.05°), which differs from β = 91.32° reported by Capitani and Mellini (2004). The calculated a value is 42.23 Å (±0.05 Å), which is shorter than the corresponding parameter of the model (Capitani and Mellini 2004). The difference between β values obtained from X-ray single crystal

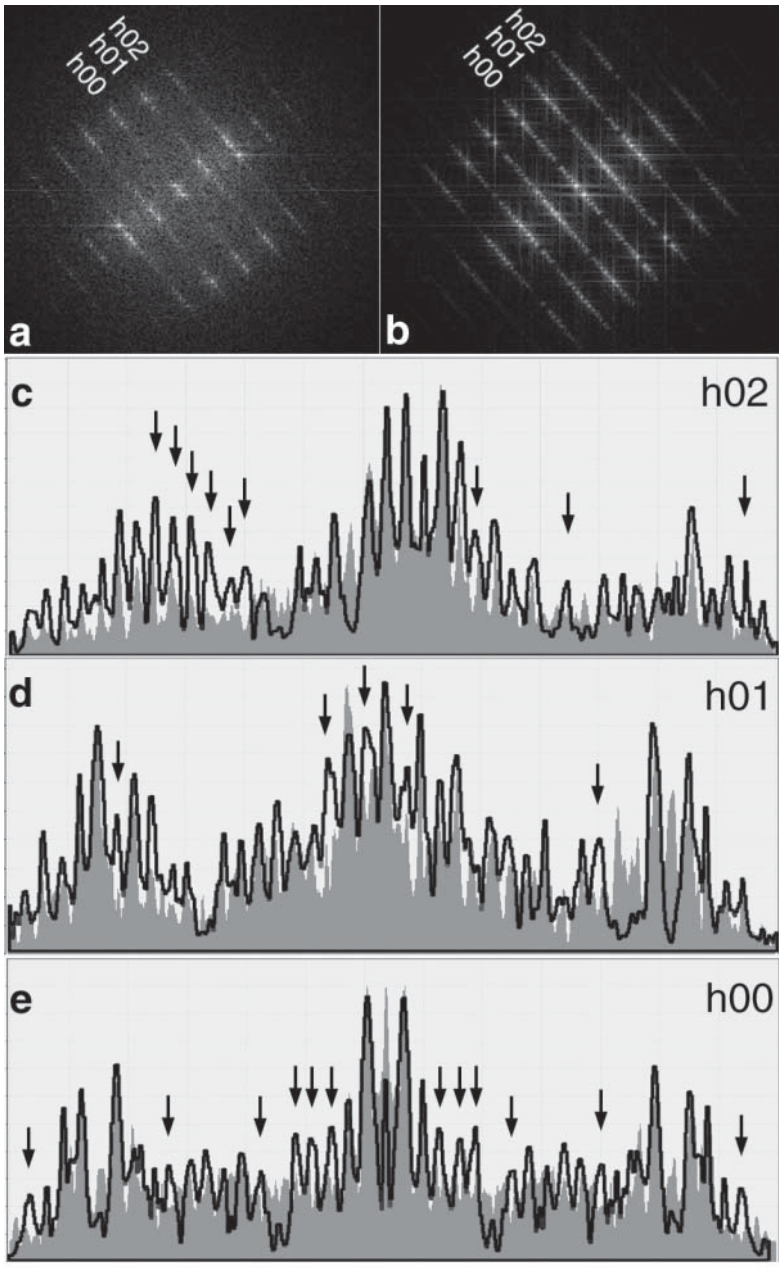

FIGURE 4. Amplitude profiles of our calculated FTs parallel to **a*** of Figures 5a and 5b of CM. (**a**) FT of Figure 5a in CM. (**b**) FT of Figure 5b in CM. (**c–e**) Amplitude profiles along the rows of $h0l$ components in **a** and **b**. The shaded regions and the black curves represent amplitudes for Figures 5a and 5b, respectively, of CM. Examples of significant differences between the FT of experimental and filtered images are indicated by arrows.

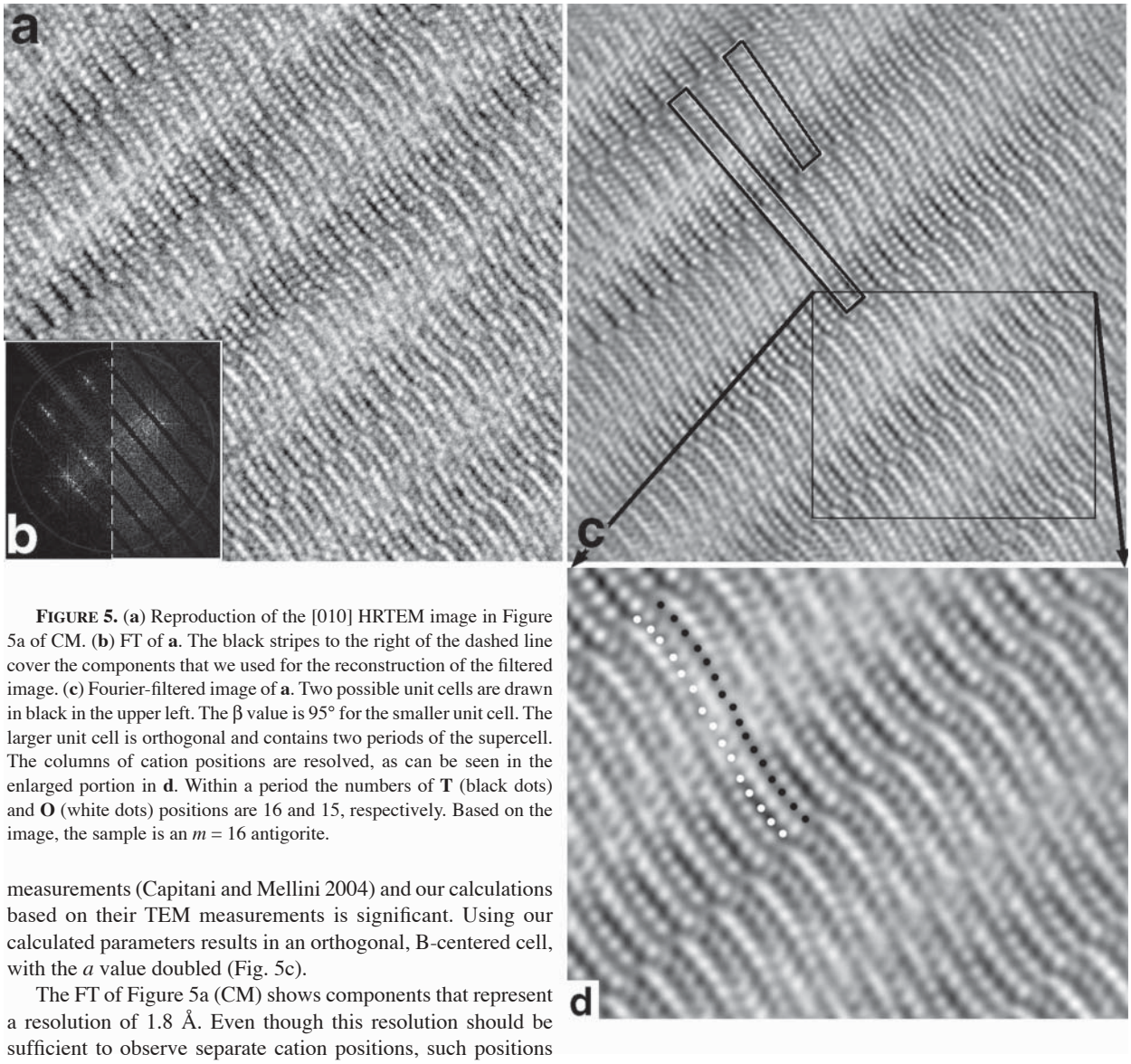

FIGURE 5. (**a**) Reproduction of the [010] HRTEM image in Figure 5a of CM. (**b**) FT of **a**. The black stripes to the right of the dashed line cover the components that we used for the reconstruction of the filtered image. (**c**) Fourier-filtered image of **a**. Two possible unit cells are drawn in black in the upper left. The β value is 95° for the smaller unit cell. The larger unit cell is orthogonal and contains two periods of the supercell. The columns of cation positions are resolved, as can be seen in the enlarged portion in **d**. Within a period the numbers of **T** (black dots) and **O** (white dots) positions are 16 and 15, respectively. Based on the image, the sample is an $m = 16$ antigorite.

measurements (Capitani and Mellini 2004) and our calculations based on their TEM measurements is significant. Using our calculated parameters results in an orthogonal, B-centered cell, with the *a* value doubled (Fig. 5c).

The FT of Figure 5a (CM) shows components that represent a resolution of 1.8 Å. Even though this resolution should be sufficient to observe separate cation positions, such positions are not resolved in the reconstructed image of CM. We Fourier filtered the image by applying masks in the form of stripes along reciprocal lattice rows parallel to **a***. This procedure guarantees the involvement of all Fourier components in the reconstruction, and does not generate extra components. Thus, the result makes it possible to locate and count the cation positions in unit cells (Fig. 5c). Using our reconstruction, additional information can be obtained about the structure of this sample.

The dark dots that represent projected columns of **T** and **O** cations are distinct (Fig. 5c). According to our image simulations and experience with other serpentine samples, the **O** sheet is darker than the **T** sheet for a wide range of defocus and sample thicknesses in HRTEM images (Dódony and Buseck 2004a). Also, **T** positions appear as dots, whereas **O** sites are more oval (Dódony and Buseck 2004b). The number of **T** and **O** positions along an **a** period are 16 and 15, respectively (Fig. 5d). This crystal is an m = even ($m = 16$) polysome, rather than the odd ($m = 17$) antigorite polysome reported by CM.

[001] projections: the question of offsets of T and O sheets and 8-reversals

In the Kunze (1958) model, both **T** and **O** sheets of the subcell are in offset positions along reversals. The antigorite model of Uehara and Shirozu (1985) and Capitani and Mellini (2004) consists of continuous **O** sheets and **T** sheets inverted periodically, with offsets only in the **T** sheets at every second reversal. In contrast, our models show offsets only in the **O** sheets (and located at every second reversal of the adjoining **T** sheets). Thus, offsets in antigorite [001] HRTEM images are common to all models although their positions differ. We wish to determine the validity of these models, whether such offsets really exist and, if they do, in which sheets they occur.

Offsets of type *b*/2 in the {110} subcell planes of the **T** sheets would provide proof of the existence of 8-reversals. Based on the offsets in their images, CM interpreted their results as evidence for the existence of 8-reversals. Their calculated images show

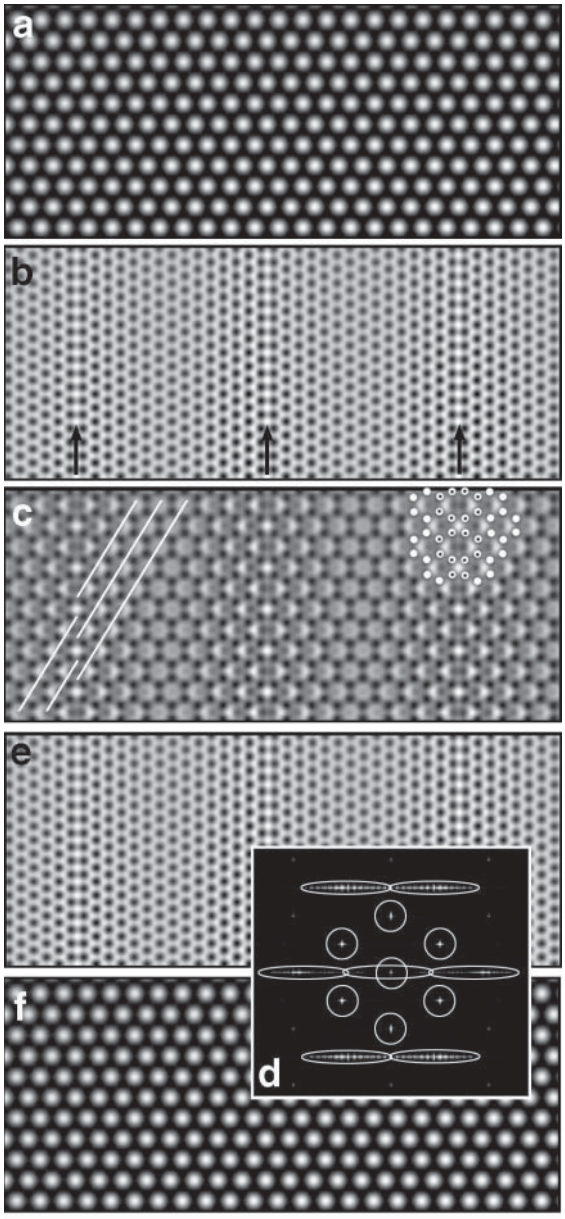

FIGURE 6. Virtual offsets in model [001] images for antigorite sheets. (**a**) Image of a **T** sheet without an 8-reversal. (**b**) Image of an **O** sheet containing offsets (arrowed). (**a**) and (**b**) were calculated for the model of Dódony et al. (2002) using experimental conditions that were applied by CM (150 Å crystal thickness, 500 Å objective defocus, and the optical parameters of a JEOL 2010 TEM) (**c**) Image showing offsets as a result of superposition of **a** and **b**. The image could be interpreted as an antigorite with 8-reversals. The hexagonal rings seem to correspond to the **T** positions. Some of these positions are marked by white dots, and those that resemble 8-membered rings with additional small black dots. (**d**) FT of **c**. The {020} and {110} components are circled, whereas {200} and {130} with their accompanying superlattice components are in the ovals. (**e**) Image of the **O** sheet, reconstructed by inverse Fourier transformation using components in ovals in **d**. (**f**) Image of the **T** sheet, reconstructed by inverse Fourier transformation using the circled components in **d**. Note that the images in **a** and **f**, as well as in **b** and **e** appear identical.

that 8-membered silicate rings should be visible even at moderate resolution (2.5 Å) in samples thinner than 300 Å. Offsets are evident in their Figure 8 and seem to be the only TEM evidence that might contradict our models. However, we have obtained similar images that show apparent offsets (e.g., Figs. 5, 7, and 21 in Dódony et al. 2002, and Fig. 16 in Dódony and Buseck 2004a), but they are not *b*/2 offsets of {110} subcell planes. In fact, we found no evidence for such offsets. Instead, we found

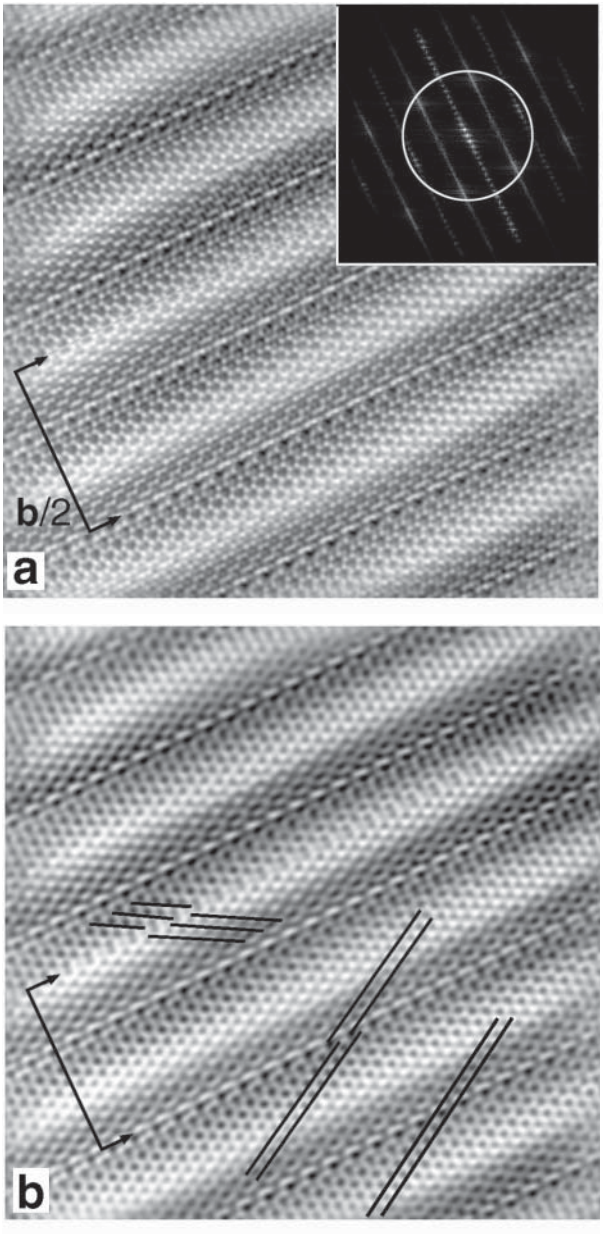

FIGURE 7. (**a**) Figure 9a from CM—an [001] antigorite HRTEM image that we sheared by *b*/2 at places indicated by arrows. Its FT is in the inset. The width of the offset slab is shown by the line between the arrows. (**b**) Image obtained by Fourier reconstruction using components in the white circle in **a**. The {110} planes (thin black lines) are now offset only where we sheared the image.

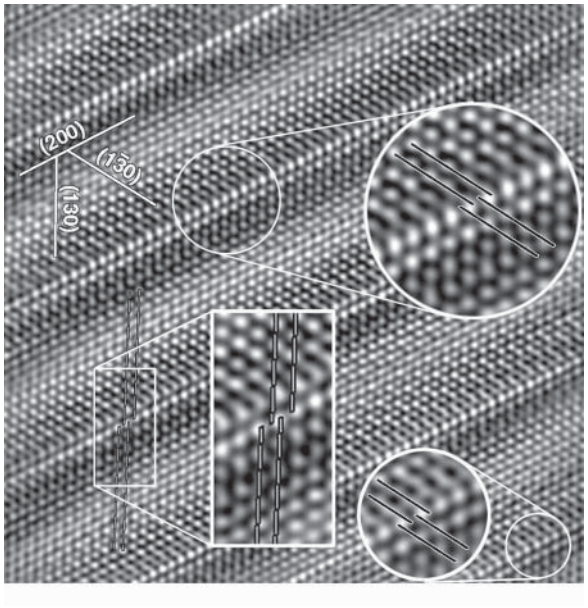

FIGURE 8. Fourier-filtered image of Figure 8a of CM. The contrast is dominated by the subcell {200} and {130} planes that are representative of the **O** sheet. The enlarged areas highlight arrangements that differ from the (pseudo)hexagonal motif characteristic of **O** sheets free of offsets. There is one plane in each unit cell along which the {130} planes are offset, as shown by the inserted enlargements. This type of offset is inconsistent with the model of Uehara and Shirozu (1985) and Capitani and Mellini (2004), but it matches our antigorite models (Dódony et al. 2002).

{110} subcell planes to be continuous and concluded that 8-reversals are lacking.

Since the **O** sheet has a shorter subcell periodicity (<2.7 Å) than the **T** sheet (~4.6 Å), the **O** sheet does not contribute to *hk*0 reflections that have d > 2.7 Å. Therefore, to see the features of the **T** sheet undisturbed by effects caused by the **O** sheet, we can either obtain reduced-resolution (~4 Å) images or generate such images by Fourier filtering (Dódony et al. 2002).

The utility of Fourier filtering for analyzing structural details of antigorite is illustrated by Figure 6. We generated images on the basis of our models (Dódony et al. 2002), with a lack of offsets in the **T** sheets (Fig. 6a) and the presence of offsets in the **O** sheets (Fig. 6b). We combined the two images by adding the density values of their corresponding pixels; the result is shown in Figure 6c. In the same way as we did with previous HRTEM images (e.g., Fig. 7 in Dódony et al. 2002), the image in Figure 6c can be decomposed into its **T** and **O** sheets by Fourier filtering. By selecting (020)- and (110)-type components in the FT, the reconstruction results in exactly the same image as the one in Figure 6a, whereas the same procedure using (200)- and (130)-type components results in the same image as in Figure 6b. The above procedure shows that Fourier filtering can be used to determine the structural details of both **T** and **O** sheets.

In spite of starting with a lack of **T**-sheet offsets, the image in Figure 6c exhibits offsets similar to those in Figures 8c, 8d, and 9 of CM. Inverting the contrast or changing the brightness in the starting images does not affect the existence of offsets in the resulting composite image. This experiment with Figure 6 shows that offsets in the **O** sheet alone can produce discontinuities in HRTEM images along the lines of reversals, without the need

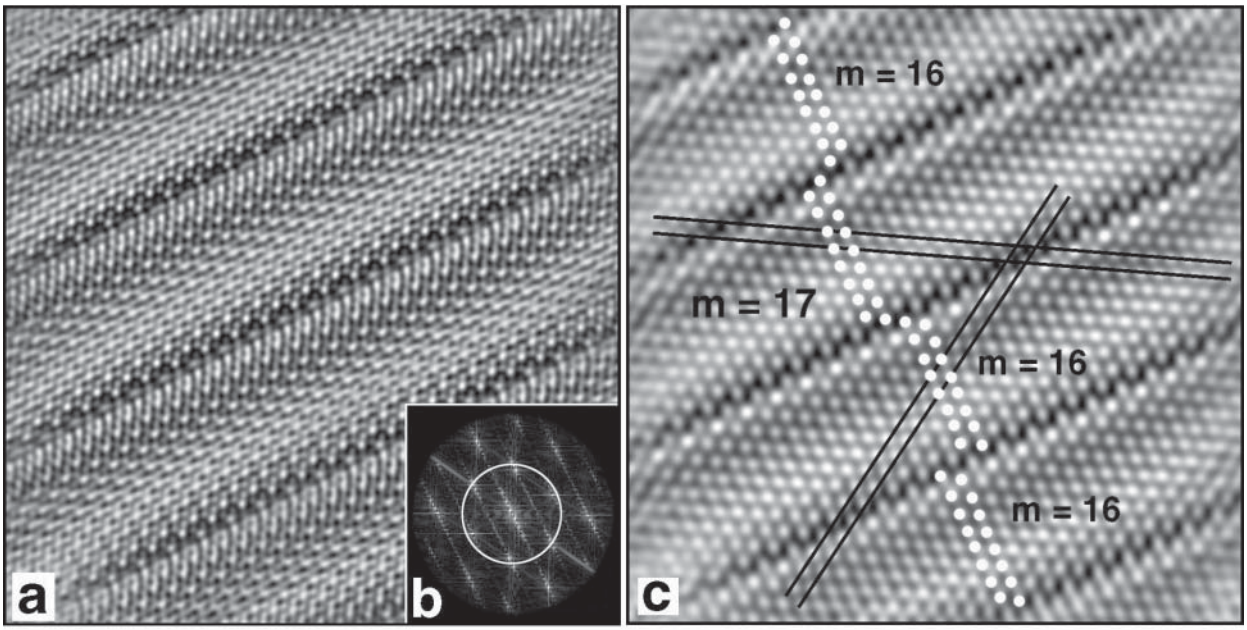

FIGURE 9. (**a**) Figure 8c from CM—an [001] antigorite HRTEM image. (**b**) FT of **a**. (**c**) Reconstructed image of **a** using Fourier components within the circled area in **b**. The continuous thin black lines show there is no offset in the {110} subcell planes. The white dots mark positions of hexagonal silicate rings. The clearly visible {110} subcell planes (parallel to the thin black lines) reveal the numbers of **T** positions in a period. The imaged area consists mostly of $m = 16$ antigorite, with one $m = 17$ unit.

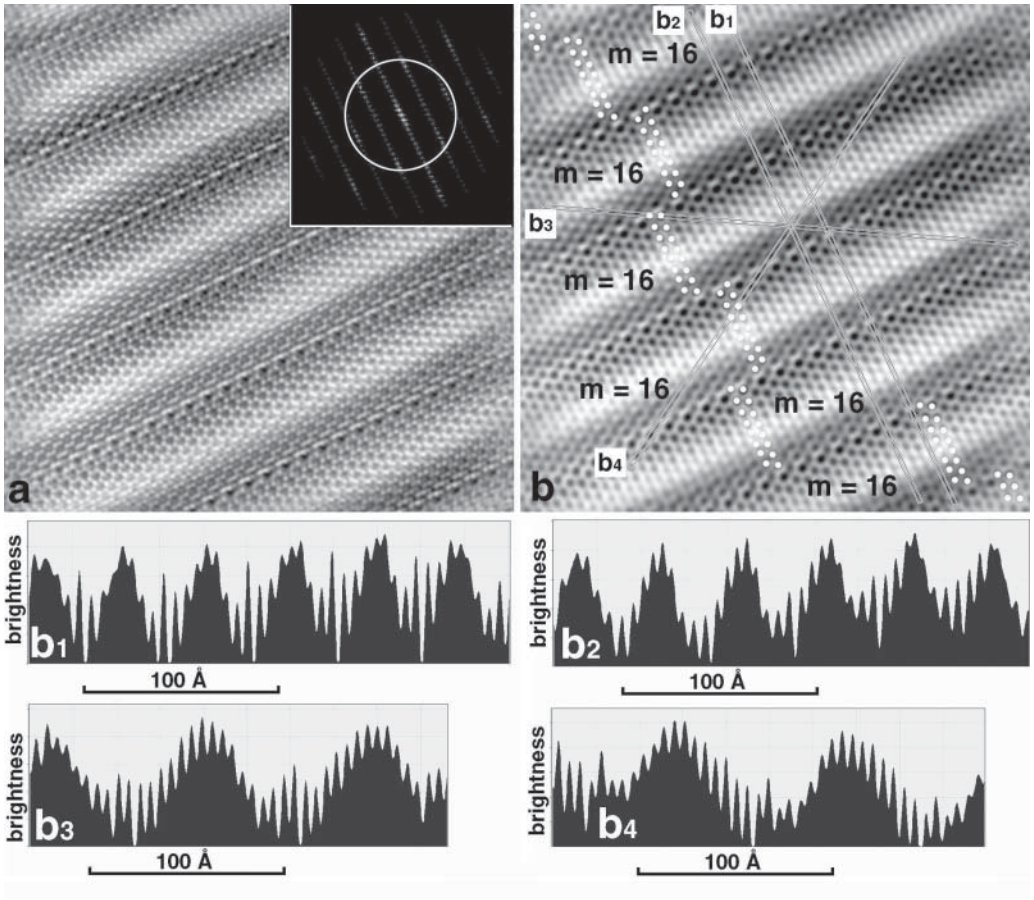

FIGURE 10. (**a**) Figure 9a from CM—an [001] antigorite HRTEM image, with its FT in the inset. Based on the FT, the estimated resolution is about 2 Å, and the HRTEM image reveals an unfaulted structure. (**b**) Reduced-resolution image of **a** using components of its FT from within the central black circle. The white dots mark positions of hexagonal silicate rings within this sample of *m* = 16 antigorite. The straight strips parallel to the {020} (b_1, b_2) and {110} (b_3, b_4) planes indicate an absence of offsets in the {110} subcell planes. Density traces integrated for their width and along strips b_1 to b_4 are shown at the bottom of the figure.

for an offset of the **T** sheet. Thus, the offsets observed by CM do not provide compelling evidence for the presence of 8-reversals in the antigorite structure.

We checked the reliability of Fourier filtering for the recognition of *b*/2 offsets in subcell {110} planes. We generated *b*/2 displacements in CM Figure 9a along lines of white dots that mark the positions of the assumed 8-reversals and midway between these lines (our Fig. 7a). This procedure resulted in offsets in the filtered image (our Fig. 7b). If the positions where our shearing occurred would have had different ring configurations prior to shearing, then they would also differ after shearing, i.e., 6-membered rings would become 8-membered and visa-versa. However, that is not what we observed. Instead, similar offsets occur in both sheared regions (our Fig. 7b). This result means that the tetrahedral configurations along the two lines are the same and shows that the **T** sheet does not contain 8-reversals.

Figure 8 can be used to infer the **O** positions. It is a processed image of Figure 8a (CM), Fourier-filtered for 2.5 Å resolution. The subcell {200} and {130} planes are clearly visible. In general, the arrangements of **O** positions are the same as the arrangements of the intersections of (200) and {130} subcell planes. A definite offset exists in the arrangement of the **O** positions. However, the antigorite models of Uehara and Shirozu (1985) and Capitani and Mellini (2004) do not have offsets in the **O** sheets, and the model of Kunze (1958) requires two offsets in an **a** period. Our antigorite models (Dódony et al. 2002) are the only ones that produce simulated images that match the observed **O** offsets.

We Fourier filtered all other [001] HRTEM images in CM and found no evidence for b/2 offsets in the {110} subcell planes and thus no indications of 8-reversals in the T sheets. The reduced-resolution image of Figure 8c (CM) shows both the lack of offsets and the number of tetrahedra (m value) in the unit cells (Fig. 9). The imaged area is inhomogeneous and consists of one m = 17 slab between m = 16 slabs. Instead of the expected m = 17 structure (Capitani and Mellini 2004), assuming that their images are representative of this crystal, it is clear that it is mainly an m = even antigorite. The other two [001] HRTEM images in CM (CM Figs. 8d and 9a) are pure m = 16 structures (Fig. 10), although CM use the m = 17 model for their interpretation. The brightness profiles along strips labeled b_1 to b_4 in Figure 10b demonstrate the offset-free, continuous, periodic {110} and {020} planes across several unit cells, again showing the lack of 8-reversals. The results of this study, which show that antigorite contains only 6-membered rings of tetrahedra at the polarity reversals of the **T** sheet and that offsets occur in the **O** rather than the **T** sheet, highlight the dangers of certain procedures used in image processing for the interpretation of HRTEM images. Much care is required to avoid producing misleading results obtained through image processing.

ACKNOWLEDGMENTS

We thank Giancarlo Capitani and Marcello Mellini for kindly sending a preprint of their manuscript. We also thank Bob Downs for reviewing an early draft and Bertrand Devouard and an anonymous reviewer for their comments. Financial support came through grants EAR-0003533 and -0440388 from the Earth Sciences Division of the National Science Foundation.

REFERENCES CITED

Capitani, G. and Mellini, M. (2004) The modulated crystal structure of antigorite: The *m* = 17 polysome. American Mineralogist, 89, 147–159.

——— (2005) HRTEM evidence for 8-reversals in the *m* = 17 antigorite polysome. American Mineralogist, 90, 991–999.

Dódony, I. and Buseck P.R. (2004a) Serpentines close-up and intimate: An HRTEM view. International Geology Review, 46, 507–527.

——— (2004b) Lizardite-chlorite structural relationships and an inferred high-pressure lizardite polytype. American Mineralogist, 89, 1631–1639.

Dódony, I., Pósfai, M., and Buseck, P.R. (2002) Revised structure models for antigorite: An HRTEM study. American Mineralogist, 87, 1443–1457.

Grobéty, B. (2003) Polytypes and higher-order structures of antigorite: A TEM study. American Mineralogist, 88, 27–36.

Hovmöller, S. (1992) CRISP: crystallographic image processing on a personal computer. Ultramicroscopy, 41, 121–135.

Kunze, W.G. (1958) Die Gewellte Struktur der Antigorits. II. Zeitschrift für Kristallographie, 110, 282–320.

Meyer, C., Leber, M., and Krivanek, O. (1996) Digital Micrograph 2.5.7: GATAN Inc, Pleasanton, San Francisco.

Perbost, R., Amouric, M., and Olives, J. (2003) Influence of cation size on the curvature of serpentine minerals. HRTEM-AEM study and elastic theory. Clays and Clay Minerals, 51, 430–438.

Uehara, S. and Shirozu, H. (1985) Variations in chemical compositions and structural properties of antigorites. Mineralogical Journal (Japan), 12, 299–318.

MANUSCRIPT RECEIVED APRIL 25, 2005
MANUSCRIPT ACCEPTED APRIL 25, 2006
MANUSCRIPT HANDLED BY BERTRAND DEVOUARD